

Proximity Effects between Superconducting and Magnetic Films

J. J. HAUSER, H. C. THEUERER, AND N. R. WERTHAMER

Bell Telephone Laboratories, Murray Hill, New Jersey

(Received 13 September 1964)

Superimposed normal-superconducting films can be used in conjunction with theory to investigate the nature and magnitude of the electron-electron interaction taking place in the normal metal. We report studies in which the normal metals were various types of magnetic materials: the ferromagnets Fe, Ni, and Gd; antiferromagnetic Cr; and the dilute magnetic alloys 1% Fe in Mo and 2.9% Gd in Pb (the last actually being a low-transition-temperature superconductor). The superconducting metal in all cases was pure Pb. Measurements of the transition temperature of the sandwich as a function of Pb film thickness were compared with a combined theory incorporating the de Gennes-Werthamer calculation of the proximity effect in nonmagnetic materials together with the Abrikosov-Gor'kov model of superconductivity in dilute magnetic alloys. Agreement for the alloy systems was satisfactory with no adjustable parameters, while extension of the theory to the concentrated, ordered systems with one parameter adjusted was qualitatively reasonable. Certain aspects of superimposed films in general were also studied: Diffusion of one metal into the other during and after deposition; dependence of the sandwich transition temperature on the order of deposition of the component films; recrystallization at room temperature; and interfacial cell reactions, selectively oxidizing one of the components at room temperature in ambient atmosphere.

I. INTRODUCTION

PREVIOUS experiments¹⁻⁷ have studied the proximity effect of a normal metal in contact with a superconductor. Various theories for the superconducting transition temperature of the resulting sandwich have been proposed,⁸⁻¹⁰ but the theory which is rooted most firmly in a fundamental microscopic basis and which seems best able to explain the experimental observations is that due to de Gennes and Werthamer.^{7,11-13} This latter theory has been verified in detail for the particular case where the "normal" metal was actually another superconductor (aluminum) with a lower transition temperature than the reference superconductor (lead).¹⁴ On the other hand, comparatively little attention has been paid so far to the proximity effect of magnetic elements in general, and ferromagnetic elements in particular. The early work of Meissner¹ on films of iron, nickel, cobalt, chromium, etc., is unreliable since the films were deposited at high temperature, allowing interdiffusion² of the two metals. Furthermore, the resistivities of the component films were not controlled. P. and R. Hilsch⁵ studied Pb-Cr and Pb-Mn couples and did not report any special effect due to the

antiferromagnetic behavior of these elements. Woolf and Reif,¹⁵ on the other hand, found that only 15 Å of Fe on 500 Å of In was sufficient to eliminate completely the superconducting gap in the energy spectrum and that 15 Å of Mn on 3000 Å of Sn smeared out the density of states considerably. The theory of the proximity effect, taking into account the magnetic properties of the component metals, has similarly been neglected. De Gennes and Sarma,^{13,16} however, have suggested that the penetration of superconducting electron pairs into a ferromagnet would be very small.

Superimposed-films experiments have generally been subjected to various criticisms as a number of metallurgical and chemical processes can occur which obscure the proximity effect being studied. When films are deposited at room temperature or above, interdiffusion and annealing effects can take place, which change the mean free path in the vicinity of the interface and thereby alter the transition temperature of the sandwich.^{3,13,17,18} Bergmann *et al.*,¹⁹ have shown that diffusion at a given temperature is more rapid the lower the temperature of deposition of the sandwich since this leads to a greater defect density. The dependence of the sandwich transition temperature on the order in which the component films are deposited was first pointed out by Hilsch⁵ on the Pb-Cu system and found again in the Pb-Pt system.⁷ This effect which we shall term irreversibility was ascribed tentatively^{7,13} to a thin oxide layer between the two films.

The experimental investigation to be reported here can be divided into two parts. In the first part, the undesirable processes such as diffusion, annealing, and interfacial oxide layer formation will be re-examined.

¹ H. Meissner, Phys. Rev. **117**, 672 (1960); IBM J. Res. Develop. **6**, 71 (1962).

² P. H. Smith, S. Shapiro, J. L. Miles, and J. Nicol, Phys. Rev. Letters **6**, 686 (1961).

³ A. C. Rose-Innes and B. Serin, Phys. Rev. Letters **7**, 278 (1961).

⁴ W. A. Simmons and D. H. Douglass, Jr., Phys. Rev. Letters **9**, 153 (1962).

⁵ P. Hilsch, Z. Physik **167**, 511 (1962).

⁶ P. Hilsch and R. Hilsch, Z. Physik **180**, 10 (1964).

⁷ J. J. Hauser, H. C. Theuerer, and N. R. Werthamer, Phys. Rev. **136**, A637 (1964).

⁸ R. H. Parmenter, Phys. Rev. **118**, 1173 (1960).

⁹ L. Cooper, Phys. Rev. Letters **6**, 698 (1961).

¹⁰ D. H. Douglass, Phys. Rev. Letters **9**, 155 (1962).

¹¹ P. G. de Gennes and E. Guyon, Phys. Letters **3**, 168 (1963).

¹² N. R. Werthamer, Phys. Rev. **132**, 2440 (1963).

¹³ P. G. de Gennes, Rev. Mod. Phys. **36**, 225 (1964).

¹⁴ J. J. Hauser and H. C. Theuerer, Phys. Letters **14**, 270 (1965).

¹⁵ M. A. Woolf and F. Reif, Phys. Rev. **137**, A557 (1965).

¹⁶ P. G. de Gennes and G. Sarma, J. Appl. Phys. **34**, 1380 (1963).

¹⁷ G. J. Van Gorp, Phys. Letters **5**, 303 (1963).

¹⁸ H. L. Caswell, Phys. Letters **10**, 44 (1964).

¹⁹ G. Bergmann, R. Hilsch, and G. V. Minnigerode, Z. Naturforsch. **19a**, 580 (1964).

In particular, a new deposition apparatus which assures the absence of an interfacial oxide layer in composite films will be described. An additional new effect, an electrochemical cell reaction between the two component metals of the sandwich has been discovered and its consequences will be discussed. In the second part, the proximity effect on superconducting lead of various magnetic materials will be studied, and a theory will be presented to explain the observations.

II. EXPERIMENTAL PROCEDURE

The data shown on the Pb-Pt and Pb-Fe systems were obtained in the getter-sputtering apparatus previously described.^{7,14} In that apparatus, after the deposition of the first film, the sputtering was discontinued in order to change sputtering electrodes. This opened the anodic can to the surrounding atmosphere of the bell jar for a few seconds. The film first deposited remained in the anodic can for about ten minutes, the time necessary to presputter the second electrode before the deposition of the second film on top. In order to prevent this delay and the resulting exposure to a relatively contaminating atmosphere, a new getter-sputtering apparatus was devised, as shown in Fig. 1. In this double-can, double-electrode system, each metal is sputtered in a separate can. In the presputtering stage necessary to bring the electrodes to equilibrium, the glass substrate located in the recess of the copper slide is held in the tubular region between the two cans. Being tight fitting, it thus acts as a mask. The slide is then moved into one of the cans to deposit the first film and without ever exposing the film to the outside bell-jar atmosphere, the slide is moved in a fraction of a second into the second can for the deposition of the second film of the composite. The substrate is held at 77°K during deposition and transferred under liquid nitrogen to a holder with four spring-loaded contacts. It is then kept at this temperature until measured. Typically, films are deposited using 1000 V, 2 mA which conditions are obtained with approximately 25 μ of argon. The vacuum in the bell jar before admitting the argon is about 3×10^{-7} Torr.

The superconducting transition temperature of a sandwich is measured resistively by detecting the appearance of 5×10^{-7} V using a current of a few microamperes. The normal residual resistivities of the component films of a sandwich are determined by sputtering separately each of the films on a glass substrate at 77°K. All films had surface dimensions of 1 cm \times 0.5 cm. The residual resistivity of the sandwich itself is measured at 4.2°K if the sandwich is normal at this temperature; if the sandwich is superconducting at 4.2°K, a magnetic field sufficient to destroy superconductivity is applied. Each film thickness is determined¹⁴ to within $\pm 5\%$ by timing the duration of deposition, and then calibrating the deposition by weighing a thick film. Deposition rates varied from 80 to 300 Å per minute.

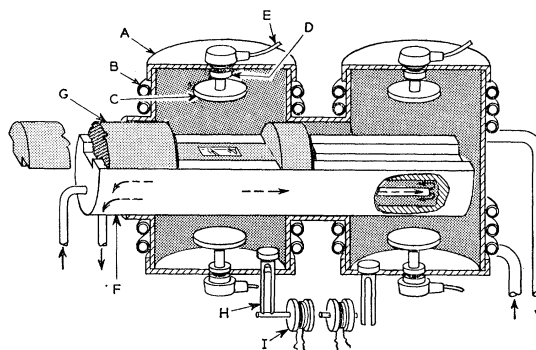


FIG. 1. Double-can-double-cathode getter-sputtering apparatus. A, Anodic can; B, cooling coils; C, cathodes; D, quartz insulators; E, cathode voltage leads; F, liquid-nitrogen cooled slide mechanism; G, substrate holder and slide; H, vents; and I, solenoidal coils for vent control.

III. METALLURGICAL AND CHEMICAL EFFECTS IN SUPERIMPOSED FILMS

A. Diffusion

When films of a composite are deposited at room temperature, interdiffusion can occur and obscure the results.^{3,17-18} In all the systems investigated here (Pb-Fe, Pb-Ni, Pb-Cr, Pb-Gd, Pb-Mo) the mutual solid solubility of lead and the other element is very restricted or negligible which already safeguards against diffusion. Furthermore, Bergmann *et al.*,¹⁹ have shown that even with low-melting-point elements evaporated at 6°K, diffusion is only appreciable above about 90°K, and that the temperature at which diffusion can take place increases with increasing deposition temperature. Consequently, since the elements investigated here are high-melting-point materials and since the temperature of measurement is below that of deposition, the likelihood of diffusion is remote.

Nevertheless, the absence of diffusion was confirmed in three different ways. Sandwiches were kept as long as three days at 77°K without any measurable change in their transition temperature (within 0.1°K) indicating no diffusion after sandwich preparation. In addition, the residual resistances of sandwiches of the Pb-Fe system are shown in Table I; since the residual resistances of a 1000-Å lead film and a 300-Å lead film are, respectively, 2.2 and 8.3 Ω while that of a 1000-Å iron film is 15.6 Ω , the resistance of the sandwiches is approximately the parallel resistance of the two component films. Similar results were observed in all the other systems investigated. A further verification of the absence of diffusion will be given after the discussion of cell reactions.

B. Interfacial Oxide Layer and Irreversibility

Irreversibility, i.e., the dependence of the transition temperature of a sandwich on the order of deposition of the metals, was first observed by Hilsch⁶ on the

TABLE I. Residual resistance and transition temperature of Pb-Fe sandwiches.

d_{Pb} (Å)	$R(\text{glass-}(1000 \text{ Å Fe})-d_{Pb})$ ohms	$T_0(\text{glass-}(1000 \text{ Å Fe})-d_{Pb})$ °K	$R(\text{glass-}d_{Pb}\text{-}(1000 \text{ Å Fe}))$ ohms	$T_0(\text{glass-}d_{Pb}\text{-}(1000 \text{ Å Fe}))$ °K
275	7.9	1.284
300	7.58	1.634	7.48	<1
325	6.6	3.164
350	6.75	4.127	6.9	1.523
375	5.9	4.068	5.9	2.332
400	5.6	2.023
412	6.1	3.412
425	5.7	3.708
450	5.4	3.752
500	4.7	5.4	4.65	4.068
550	3.96	4.5
600	3.57	5.17
700	3.17	5.97	3.0	5.5
850	2.8	5.85
1000	2.35	6.480	2.2	6.29
1200	1.73	6.51

Pb-Cu system and in Ref. 7, Fig. 3 on the Pb-Pt system. In both cases, the greatest depression in transition temperature is obtained when the lead is deposited last. Since lead is much more likely to oxidize than the noble metals, it was tempting to speculate that the irreversibility was due to the formation of an interfacial oxide layer. The effect of such a layer would be to spatially separate the two films, and thereby reduce the proximity effect.

The possibility of forming an interfacial oxide layer has now been completely eliminated with the new experimental apparatus in use. Indeed, each metal is sputtered in a double cathode getter-sputtering can, and it has been shown that such a system²⁰ produces an atmosphere with a concentration of interstitials smaller than 10^{-9} . Even if one ignores the improved atmosphere caused by getter-sputtering, it would take about 7 sec to produce an adsorbed monolayer in a bell jar with a starting vacuum of 3×10^{-7} mm. Since the transfer of the substrate from one can to the other is accomplished in a fraction of a second, the formation of a monolayer is impossible. The absence of an interfacial oxide layer in the getter-sputtering atmosphere was further demonstrated by the fact that the resistance of a 75-Å lead film remained unchanged, even though kept 1 h under a shield while sputtering was proceeding.

Contrary to expectation, however, when the Pb-Pt experiments were repeated in the new system, the same irreversibility as previously reported⁷ was again found. It now seems that the most probable explanation of this irreversibility is that the morphology and hence the resistivity of the first few layers of a deposited film depends very strongly on the type of surface where growth is initiated. In other words, irreversibility arises because it is very often impossible to meet experimentally the theoretical requirement that the film

should have a uniform mean free path throughout. This explanation is supported by the fact that thin lead films sputtered on glass, magnesium oxide, sapphire, and quartz substrates were found to have quite different resistivities. Stresses are most probably not responsible for such differences since the films were deposited at 77°K and the coefficient of thermal expansion of lead is so much greater than that of any substrate used.

Using the de Gennes-Werthamer theory¹¹⁻¹³ (the validity of which has been demonstrated on the Pb-Al system¹⁴) one can calculate the transition temperature of a sandwich versus lead film thickness at constant normal metal thickness. Using parameters appropriate to platinum deposited at 77°K ($\rho_{Pt} = 30 \times 10^{-6}$ Ω cm, $\rho_{Pb} = 18 \times 10^{-6}$ Ω cm) one obtains the upper curve of Fig. 2. Agreement is very good with the data of Ref. 7, Fig. 3, for the order of deposition glass-Pt-Pb. Consequently, when irreversibility occurs, contrary to the averaging procedure adopted by Hilsch,^{5,6} one should instead use only the data with the order of deposition giving the biggest depression in transition temperature provided the resistance of the sandwich is still approximately the parallel resistance of the two films. This point is further demonstrated by first depositing platinum on sapphire at 1000°C in order to increase its mean free path; taking ρ_{Pt} now to be 3.4×10^{-7} Ω cm, one obtains the lower curve of Fig. 2 which again is in good agreement with the data. Thus, the theoretical analysis leads us to conclude that in Fig. 3 of Ref. 7 it is the glass-Pb-Pt data which are incorrect. This may be due to the possibility that the first platinum layers which are deposited on the lead film have a very small grain size and therefore a very short mean free path. If so, then the proximity effect would be greatly reduced without affecting the resistivity of the sandwiches as a whole. Another example is the Pb-Fe system, where deposition of the iron before the lead leads to a greatly reduced depression in transition temperature without increasing the resistivity of the sandwich (Table I). The

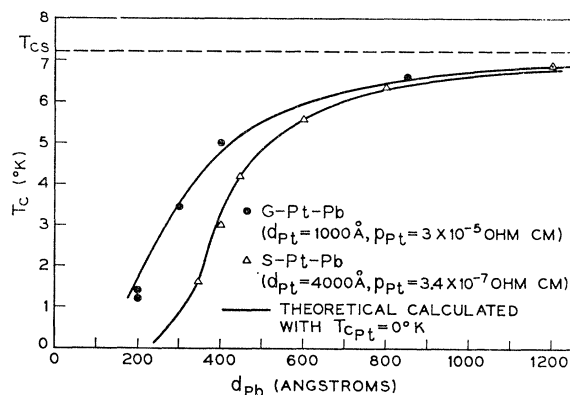


FIG. 2. Transition temperature of substrate-Pt-Pb sandwiches with a constant platinum film thickness [upper curve: 1000-Å platinum film deposited at 77°K on glass (G)—lower curve: 4000-Å platinum film deposited at 1300°K on sapphire (S)].

²⁰ J. J. Hauser and H. C. Theuerer, Rev. Mod. Phys. 36, 80 (1964).

TABLE II. Cell-reaction experiments in sandwiches warmed up to room temperature (R.T.).

Sandwich	Initial T_0 (°K)	T_0 (°K)	Hours in air at R.T.	T_0	Hours in 3×10^{-7} Torr vacuum at R.T.
(400 Å Pb)/(4000 Å Pt)	2.977	3.118	1.5
		<1.27	70
(600 Å Pb)/(4000 Å Pt)	5.6	3.287	17
(375 Å Pb)/(1000 Å Fe)	4.565	7.0	2
(25 Å Fe)/(500 Å Pb)	4.281	7.22	20
(25 Å Fe)/(500 Å Pb)	4.281	6.48	3	1.216	16
(1150 Å Ni)/(400 Å Pb)	3.134	4.8	20
(150 Å Cr)/(500 Å Pb)	4.55	7.22	0.25
		<1.33	3
(80 Å Gd)/(300 Å Pb)	2.98	7.2	0.25
		7.2	120

plausibility of this explanation was further demonstrated in the case of the Pb-Cr system where deposition of the lead on the chromium resulted again in a much reduced depression in transition temperature accompanied this time by a large increase in resistance. Since in these sandwiches the resistance measured was essentially that of the lead, one must argue that the nucleation of lead on the high-resistivity chromium resulted in the entire lead film having a small grain size rather than just the first few layers. In any event, regardless of the validity of the proposed explanation for the irreversibility, it is quite certain that, in general, the order of deposition leading to the lowest transition temperature is the correct one for the proximity effect. Of the systems studied in this paper, the Pb-Fe, Pb-Gd, and Pb-Cr systems were irreversible and the lowest transition curve was chosen to fit the theory, while the Pb-Ni system was reversible (Fig. 4).

C. Electrochemical Cell Reactions

An additional new effect, called a cell reaction was discovered in this study upon warming up the sandwiches in ambient atmosphere. This cell reaction is produced when two dissimilar metals are in contact with moisture and results in the oxidation of the most anodic metal. This reaction is very rapid in sandwiches deposited at low temperature, as such films are notoriously porous, and consequently, provide many channels for letting water molecules reach the interface. In all but two systems investigated (Pb-Al; Pb-Gd), it was always the lead which was the anodic metal and which oxidized. Since this reaction starts at the interface, the first result is to decouple the two films of the sandwich and the transition temperature returns to that of pure Pb, 7.2°K. Eventually, the entire lead film is oxidized and the transition temperature drops below detection. The cell reaction is fastest the more electronegative one element is relative to the other and the lower the sandwich deposition temperature. In the case of the Pb-Pt system, with both films deposited at 77°K, the lead film was oxidized so rapidly when the sandwich warmed up,

that it was impossible to observe the initial transition temperature increase. The cell reaction can, however, be slowed down by depositing the first film (e.g., the platinum) at high temperature. The complete cycle of the cell reaction is best demonstrated by the Pb-Cr system (Table II). The fact that the transition temperature can return to 7.2°K, the transition temperature of pure lead, provides us with a further proof of the absence of diffusion into the lead film, as all the elements here considered would, if dissolved in lead, depress its transition temperature. The initial increase in transition temperature of the sandwich is not accompanied by any appreciable increase in resistance, because only the lead in the vicinity of the interface has been oxidized. After the transition temperature has dropped below detection, the resistance of the sandwich is markedly higher, and the presence of the lead oxide has been established by electron diffraction. In the case of the Pb-Al and Pb-Gd systems, where aluminum and gadolinium are the electropositive elements which oxidize, the transition temperature increases to 7.2°K when the sandwich is warmed up and remains unchanged as shown for the Pb-Gd system in Table II. Another decoupling mechanism in sandwiches has been discussed by Miles and Smith.²¹

D. Annealing

When a sandwich is warmed up to room temperature, another phenomenon, annealing, takes place concurrently with the cell reaction. A low-melting-point metal such as lead is known to recrystallize at room temperature, and this in turn should effect the sandwich transition temperature. These two phenomena have been separated by an experiment conducted on a 25 Å Fe/500 Å Pb sandwich. Such a sandwich has a transition temperature of 4.28°K and a residual resistance of 4.65 Ω (Tables I and II, Fig. 3). After holding the film for 16 h under vacuum at room temperature (which eliminates the cell reaction by eliminating

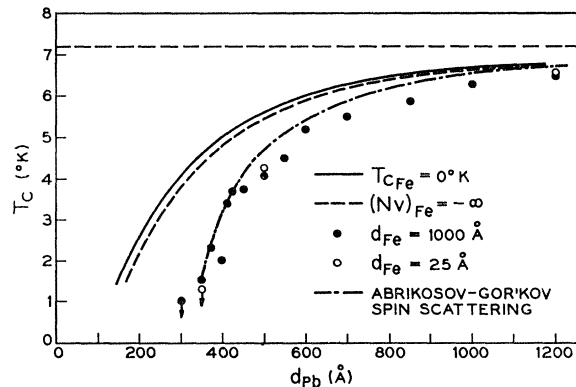


FIG. 3. Transition temperature for glass-Pb-Fe sandwiches with a constant iron film thickness of 1000 Å.

²¹ J. L. Miles and P. H. Smith, J. Appl. Phys. 34, 2109 (1963).

moisture) the residual resistance had decreased to 1.2Ω owing to annealing of the lead film. This fourfold increase in the mean free path of the lead resulted in a much more pronounced proximity effect, the transition temperature falling to 1.22°K . After warming up this sandwich in air for 3 h the transition temperature increased to 6.48°K as a result of the cell reaction. Thus, with the variety of metallurgical and electrochemical effects taking place, a transition-temperature measurement of a sandwich exposed at any time to room temperature must be regarded as completely unreliable.

IV. PROXIMITY EFFECT OF LEAD WITH MAGNETIC MATERIALS

A. Ferromagnets

The most interesting materials to be considered from the point of view of a proximity effect are the ferromagnetic elements, as it seems to be true that strong ferromagnetism and superconductivity are mutually exclusive. The results on the three ferromagnetic elements: iron, nickel, and gadolinium are shown, respectively, in Figs. 3, 4, and 5. In order to interpret these results theoretically, we might first of all ignore the fact that they are ferromagnetic and apply to them the de Gennes-Werthamer theory.¹¹⁻¹³ The three equations¹⁴ which give an implicit solution for the transition temperature of the sandwich as a function of the thickness d_s and d_n , of the superconducting and normal films, respectively, are

$$\ln T_{cs}/T_c = \chi(\xi_s^2 k_s^2) \quad (1)$$

$$\ln T_{cn}/T_c = \chi(-\xi_n^2 k_n^2), \quad (2)$$

$$[N\xi^2 k \tanh kd]_s = [N\xi^2 k \tanh kd]_n, \quad (3)$$

where $\chi(z) = \Psi(\frac{1}{2} + \frac{1}{2}z) - \Psi(\frac{1}{2})$ and Ψ is the digamma function. Here T_{cs} , T_{cn} and T_c are the transition temperatures of the superconductor, the normal metal, and the sandwich, respectively; and ξ is the effective co-

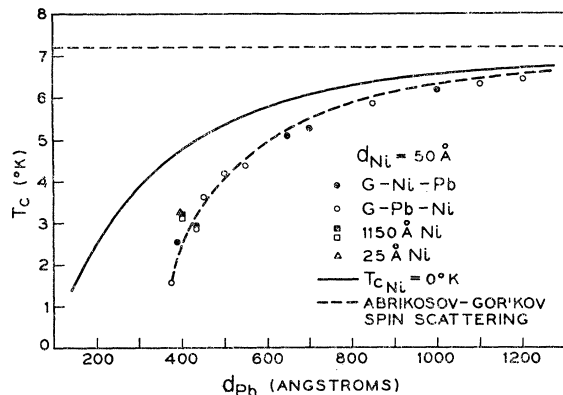


FIG. 4. Transition temperature for glass-Ni-Pb and glass-Pb-Ni sandwiches with a constant nickel film thickness of 50 \AA .

herence length defined as

$$\xi = (\pi \hbar k_B \sigma / 6 T_c e^2 \gamma)^{1/2}, \quad (4)$$

where σ is the low-temperature conductivity and γ the coefficient of normal electronic specific heat; and N is the density of states at the Fermi surface, assumed to be proportional to γ . In all experiments performed in this study $\rho_{\text{Pb}} = 1.5 \times 10^{-5} \Omega \text{ cm}$ and²² $\gamma_{\text{Pb}} = 1.72 \times 10^8 \text{ ergs/cc } ^\circ\text{K}^2$.

Beginning with the case of iron, we may first assume that its transition temperature is $T_{c \text{ Fe}} = 0^\circ\text{K}$. Taking the values $\rho_{\text{Fe}} = 1.11 \times 10^{-4} \Omega \text{ cm}$ and²² $\gamma_{\text{Fe}} = 7.1 \times 10^8 \text{ ergs/cc } ^\circ\text{K}^2$, we combine Eqs. (1)–(4) to yield the solid curve in Fig. 3. The data lie considerably below this curve. Attempting to obtain better agreement, we may next try the hypothesis that iron has an effective electron-electron interaction which is infinitely repulsive

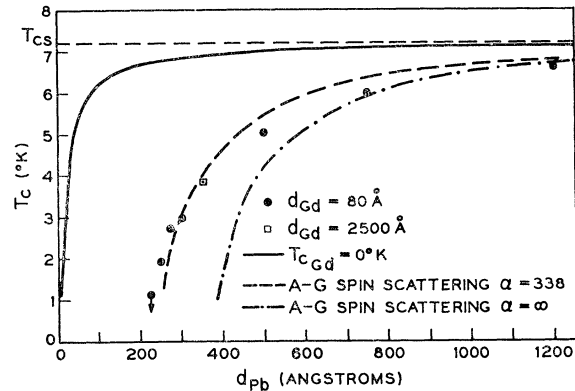


FIG. 5. Transition temperature for glass-Pb-Gd sandwiches with a constant gadolinium film thickness of 80 \AA .

instead of zero. This may be inserted into Eq. (2) via the BCS relation

$$\ln 1.14 \Theta_D / T_{cn} = 1 / NV = 0, \quad (5)$$

where Θ_D is the Debye temperature (467°K for iron). Hypothesis (5), together with Eqs. (1)–(4), now lead to the dashed curve of Fig. 3, which is little changed from the previous curve for $NV = 0$ and still in disagreement with the measurements. We are forced to conclude that the ferromagnetism of the iron plays an important role in determining the sandwich transition temperature.

Abrikosov and Gor'kov (AG),²³ and later de Gennes and Sarma,¹⁶ have investigated theoretically the effect on a superconductor of a dilute concentration of randomly oriented and distributed paramagnetic impurities. It was found that such impurities sharply reduce the transition temperature, because of the differing exchange potentials felt by the up and down

²² C. Kittel, *Introduction to Solid State Physics* (John Wiley & Sons, Inc., New York, 1957), p. 259.

²³ A. Abrikosov and L. P. Gor'kov, *Zh. Eksperim. i Teor. Fiz.* 39, 1781 (1960) [English transl.: *Soviet Phys.—JETP* 12, 1243 (1961)]. This paper will be referred to as (A-G).

spin electrons comprising the correlated electron pairs. The reduction of T_c below the pure value T_{cs} is described by the equation

$$\ln T_{cs}/T_c = \chi(\hbar/2\pi\tau_s k_B T_c), \quad (6)$$

where τ_s is the electron relaxation time. The application (at first glance inappropriate) of this model of dilute, random spin impurities to the situation at hand of ferromagnetic iron suggested itself for two reasons. Firstly, because of the low deposition temperatures, the iron films have a very small grain size, and thus their magnetic structure is one of many small, randomly oriented domains. Secondly, the recent theoretical work of Gor'kov and Rusinov²⁴ indicates that the effect on T_c of the ferromagnetic order within a domain might be approximated at least crudely via Eq. (6) with an altered definition of τ_s . Furthermore, a completely reliable theory for superconductivity in a concentrated ferromagnet does not yet exist. Noting the functional similarity of Eqs. (2) and (6), it is perhaps not surprising that an analysis combining the proximity effect with the (AG) model of dilute, random spin impurities leads to the replacement for Eq. (2)

$$\ln T_{cn}/T_c = \chi[-\xi_n^2 k_n^2 + (\hbar/2\pi\tau_s k_B T_c)]. \quad (7)$$

A brief sketch of the derivation of this equation is given in the Appendix.

The modified Eq. (7) now contains an unknown parameter τ_s . We choose the value $T_{cFe} = 0^\circ\text{K}$, having learned that the theory is comparatively insensitive to this quantity, and determine τ_s by fitting to the experimental point $d_{Pb} = 350 \text{ \AA}$, $T_c = 1.52^\circ\text{K}$. The resulting value of $\tau_s = 1.2 \times 10^{-14}$ sec is not unreasonable; taken with a nominal Fermi velocity of 10^8 cm/sec it implies a spin scattering length of 120 \AA , which is to be compared with a grain size of roughly 50 \AA . With τ_s thus fixed, Eqs. (1), (3), (4), and (7) combine to give the lower curve of Fig. 3, which is in fair agreement with the data. The fit is comparatively insensitive to the choice of τ_s ; the extreme value $\tau_s = 0$ leads to a curve similar to the lower one of Fig. 3, but displaced by 45 \AA greater lead thickness. In the limit of $\tau_s = 0$, Eqs. (1), (3), (4), and (7) are replaced by a single equation which no longer depends on the normal-film properties:

$$\ln T_{cs}/T_c = \chi(\pi^2 \xi_s^2 / 4d_s^2). \quad (8)$$

It is instructive to use Eq. (7) to obtain k_n^{-1} , which is a measure of the depth of penetration of superconducting pairs into the normal metal. Defining $\alpha = \hbar/2\pi\tau_s k_B T_{cs}$ and choosing $T_{cn} = 0^\circ\text{K}$, one obtains in the limit of large α :

$$k_n^{-1} = \xi_{ns} / (\alpha)^{1/2}, \quad (9)$$

where $\xi_{ns} = \xi_n(T = 7.2^\circ\text{K})$. Relation (9) shows that

TABLE III. Transition temperature and residual resistance for glass-(500 Å Pb)- d_{Fe} sandwiches.

d_{Fe} (Å)	T_c (°K)	$R(4.2^\circ\text{K}, 17.4 \text{ kG})$ (Ω)
1000	4.068	4.65
50	4.035	4.75
25	4.281	4.12
10	4.55	4.11
4	4.89	4.50

when α is large, i.e., for strong magnetism, k_n^{-1} is temperature independent and small. Whereas Eq. (2) implies that k_n^{-1} should vary from 23 \AA at 7.2°K , up to 50 \AA at 1.5°K if iron were nonmagnetic, the large value of $\alpha (= 14)$ produces the result $k_n^{-1} = 6 \text{ \AA}$ and independent of temperature. Taking note of Eq. (3), we conclude that the full depression of the transition temperature is attained when the iron is only about 15 \AA thick. This prediction is partially verified by the result, illustrated in Fig. 3, that the effects of a 1000-\AA iron film are identical to those of a 25-\AA film. A more conclusive check is hampered by the fact that iron films thinner than 25 \AA are no longer continuous (the resistance increases by a factor of the order of 10^6 between 50 and 25 \AA). When the iron film thickness is reduced below 25 \AA , the nominal thicknesses shown in Table III only represent averages, and the reduction of the depression in transition temperature is due to the fact that the lead film is only partially covered by iron islands.

The Pb-Ni and Pb-Gd systems are similar to the Pb-Fe system just discussed. Again assuming $T_{cn} = 0^\circ\text{K}$ in both cases, and taking the values $\rho_{Ni} = 1.9 \times 10^{-4} \text{ \Omega cm}^{22}$, $\gamma_{Ni} = 1.10 \times 10^4 \text{ ergs/cc } ^\circ\text{K}^2$, $\rho_{Gd} = 1.22 \times 10^{-2} \text{ \Omega cm}$, and²⁵ $\gamma_{Gd} = 3.38 \times 10^8 \text{ ergs/cc } ^\circ\text{K}^2$, the theory ignoring the ferromagnetism yields the solid curves in Figs. 4 and 5, in clear disagreement with the data. Fitting the nickel data at the point $d_{Pb} = 375 \text{ \AA}$, $T_c = 1.57^\circ\text{K}$, so that $\alpha_{Ni} = 6$, and similarly fitting the gadolinium data at $d_{Pb} = 300 \text{ \AA}$, $T_c = 3^\circ\text{K}$, so that $\alpha = 338$, we obtain the dashed curves in Figs. 4 and 5. Agreement of these curves with the data is again fair, less good for Gd than for Ni. Figure 4 illustrates that in contrast to Fe and Gd, the Pb-Ni system is reversible.

B. Antiferromagnets

We next turn our attention to a different type of magnetism, namely, to antiferromagnetic chromium. Data for the Pb-Cr system is shown in Fig. 6. Continuing to assume $T_{cn} = 0^\circ\text{K}$, and using the values $\rho_{Cr} = 3.7 \times 10^4 \text{ \Omega cm}$ and²² $\gamma_{Cr} = 2.2 \times 10^8 \text{ ergs/cc } ^\circ\text{K}^2$, the theory without magnetic effects ($\alpha = 0$) yields the solid curve of Fig. 6. If one includes the (AG) theory as was done for the ferromagnets, one obtains the dashed curve of Fig. 6 with $\alpha = 21$ by fitting at the experimental point $d_{Pb} = 275 \text{ \AA}$, $T_c = 1^\circ\text{K}$; the bottom curve for $\alpha = \infty$.

²⁴ L. P. Gor'kov and A. I. Rusinov, Zh. Eksperim. i Teor. Fiz. 46, 1363 (1964) [English transl.: Soviet Phys.—JETP 19, 922 (1964)].

²⁵ K. A. Gschneider, Jr., *Rare Earths Alloys* (D. Van Nostrand Inc., New York, 1961).

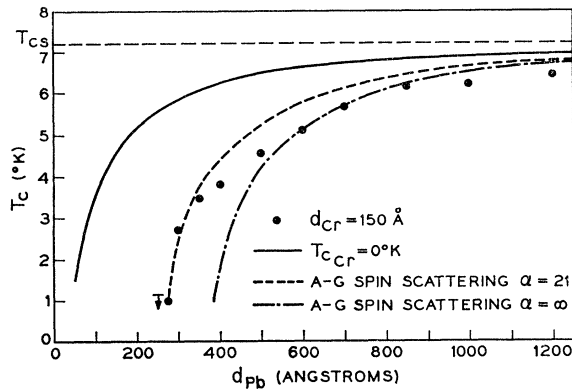


FIG. 6. Transition temperature for glass-Pb-Cr sandwiches with a constant chromium film thickness of 150 Å.

Although the general behavior of the data is accounted for by the theory, the agreement in this case is only fair. Actually, de Gennes and Sarma¹⁶ have discussed the antiferromagnetic case and remarked that the (AG) theory is not appropriate in that case, because the one electron wave functions have the Bloch form. Their argument, however, applies only to a perfect, bulk antiferromagnet; whereas in the present situation, the grain size is so small and spin scattering at domain walls sufficiently rapid that a random-impurity spin description may still be valid.

One feature that seems to be common to all four of the partially ordered magnetic systems discussed so far is that the transition temperature data lie well below the theoretical predictions for lead film thicknesses greater than 500 Å. It is tempting to envision some long-range penetration of the magnetic order into the lead as being the mechanism for the transition temperature depression of even these comparatively thick films. Evidence for such an effect in the normal state was found by hysteresis studies.²⁶ On the other hand, the small domain size of the magnetic elements would seem to rule out a penetration into the lead of the order of a distance much greater than the domain size itself. Furthermore, hysteresis measurements on Fe and Ni films, and on Pb-Fe and Pb-Ni sandwiches show that the films as made have a zero magnetic moment, a coercive force of 500 G, and a remanence of 1500 G for nickel, 9000 G for iron. These data support the view that the sandwiches are randomly oriented aggregates of small domains. Additional evidence against long-range magnetic order in lead comes from measurements of a sandwich first as made, and then after the application of a field sufficient to produce a remanence of 1000 G. The transition temperatures in the two cases were identical. Finally, a Pb-Fe sandwich deposited at 77°K in a field of 250 G was found to have a transition temperature identical to an otherwise similar sandwich

²⁶ J. C. Bruyère, O. Massenet, R. Montmory, and L. Néel, *Compt. Rend.* **258**, 841 (1964).

deposited in zero field. If there were a long-range effect of the magnetic order on the lead, it would be suspicious that the effect was not enhanced by aligning the magnetic domains.

C. Dilute Magnetic Alloys

Let us now focus on systems where the (AG) theory is supposed to apply, namely, dilute magnetic alloys. Experimental results on Pb-Mo:(1% Fe) sandwiches are shown in Fig. 7. These alloy films were produced by two different techniques: by sputtering from a Mo:(1% Fe) alloy target, and by using a molybdenum target with an iron insert. In the latter method, the ratio of the areas of iron to molybdenum, corrected by the ratio of their relative sputtering rates, was determined to yield the desired alloy concentration. This technique is particularly useful in cases where one element is insoluble in another, such as Gd in Pb, to be discussed below. Both techniques yielded the same one at.% iron concentration as determined by x-ray fluorescence analysis and atomic absorption.²⁷ The theoretical curves of Fig. 7 were calculated using $\rho_{\text{Mo:(1% Fe)}} = 1.42 \times 10^{-3} \Omega \text{ cm}$, $\rho_{\text{Mo}} = 5.37 \times 10^{-4} \Omega \text{ cm}$ and $\gamma = 2.27 \times 10^8 \text{ ergs/cc } ^\circ\text{K}^2$ for both molybdenum and the molybdenum: iron alloy. The lower curve which represents the (AG) spin-scattering theory with $\alpha = 10.7$ is in good agreement with experiments. In this case, it is possible to remove the spin effect both theoretically and experimentally by performing experiments on pure molybdenum. This is shown by the middle curve of Fig. 7 which again is in good agreement with the corresponding experiments.

It has been suggested²⁸ that a critical concentration of 200 ppm of iron would be sufficient to depress the transition temperature of molybdenum from 0.92°K

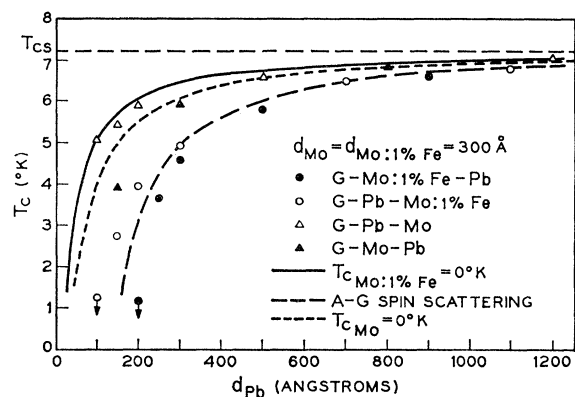


FIG. 7. Transition temperature for the Mo:1% Fe-Pb and Mo-Pb systems with constant Mo:1% Fe and molybdenum film thicknesses of 300 Å.

²⁷ We are indebted to Miss S. M. Vincent for the x-ray fluorescence analysis and to T. Y. Kometani for the atomic-absorption measurements.

²⁸ T. H. Geballe, B. T. Matthias, E. Corenzwit, and G. W. Hull, Jr., *Phys. Rev. Letters* **8**, 313 (1962).

down to zero. The critical value of τ_s necessary to accomplish this is given by setting $T_c=0$ in Eq. (6):

$$(\hbar/\tau_s)_{\text{critical}} = 1.76k_B T_{c0} \quad (10)$$

which equals half the BCS energy gap of the pure element at 0°K. This corresponds to $\alpha_{\text{crit}}=0.28$. Using this result together with the value $\alpha=10.7$ derived from the proximity effect measurements for 1% iron in molybdenum, and assuming that τ_s is inversely proportional to the impurity concentration for the dilute alloys under consideration, we arrive at a critical concentration of 260 ppm, confirming the earlier results.²⁸

De Gennes and Sarma¹⁶ have pointed out that the concept of a localized moment is obscure in the Mo:Fe system, since both the impurity and the host metal have unfilled d shells. The presence of the localized moment in these experiments was established by depositing Mo:(1% Fe) films at 1000°C and observing a resistivity minimum as reported previously.²⁹ The resistivity minimum cannot be observed in Mo:(1% Fe) films deposited at 77°K, because the spin scattering is totally overshadowed by the boundary scattering of the small grains. Thus, the proximity effect can be used to detect the presence of a localized moment in cases where the impurity can only be quenched in at low temperatures and, therefore, where other experimental detection techniques would fail.

Finally, we consider the proximity effect of lead with a dilute Pb:Gd magnetic alloy. This case is especially appealing for several reasons. First of all, the boundary condition (3) is greatly relaxed because both sides of the interface are basically the same metal, Pb. In addition, since this alloy has been previously studied,^{15,30} the value of α can be calculated directly instead of being treated as an adjustable parameter. Similarly, T_{en} can be experimentally detected, rather than guessed at. The Pb:Gd films were produced using a lead target with gadolinium inserts and the gadolinium concentration of 2.9% was determined from the ratios of areas and sputtering rates. The transition temperature of an isolated Pb:(2.9% Gd) film was 1.52°K which corresponds to a rate of depression of the transition temperature of pure lead of 196°K per unit concentration, in agreement with previous experiments.^{15,30} Using $T_c=1.52$ °K in Eq. (6) yields $\alpha=0.257$ at this concentration. The experimental results for the Pb-Pb:2.9% Gd proximity effect are shown in Fig. 8. The theoretical curves are calculated employing $\rho_{\text{Pb}}(2.9\% \text{ Gd}) = 30 \times 10^{-6} \Omega \text{ cm}$ and $T_{c \text{ Pb:}(2.9\% \text{ Gd})} = 1.52$ °K; the solid curve corresponds to $\alpha=0$, the dashed curve corresponds to the calculated value $\alpha=0.257$. The data is seen to agree quite well with the latter curve, which is now an absolute fit, without any adjustable parameters.

Consequently, the combination of the (AG) spin-

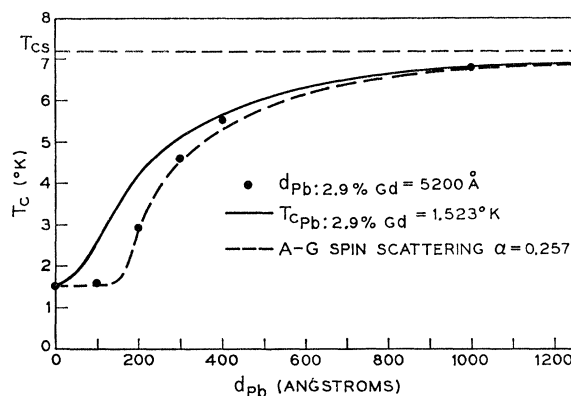


FIG. 8. Transition temperature for Pb-Pb:2.9% Gd sandwiches with a constant Pb:2.9% Gd film thickness of 5200 Å.

scattering theory together with the proximity effect theory is confirmed satisfactorily for dilute magnetic alloys. The remaining discrepancies discussed above for the magnetically ordered elements may be ascribed to a breakdown of the (AG) model when extrapolated to concentrated systems.

ACKNOWLEDGMENTS

We are indebted to D. D. Bacon for the preparation of all the superimposed films used in this study, to W. H. Haemmerle for technical assistance in obtaining the data, to D. Dorsi for arc-melting some of the electrode materials and finally to Mrs. A. M. Hunt for electron-diffraction studies of some of the films.

APPENDIX

We sketch here a derivation of Eq. (7) which combines the analysis of de Gennes¹⁸ and Werthamer¹² for the proximity effect with that of Abrikosov and Gor'kov²⁸ for the role of paramagnetic impurities. We begin with the eigenvalue equation determining the transition temperature as given by Ref. 12, Eq. (A4) [to be denoted 12:(A4)],

$$\Delta(\mathbf{r}) = V(\mathbf{r}) \int d^3r' Q(\mathbf{r}-\mathbf{r}') \Delta(\mathbf{r}'). \quad (A1)$$

Here $\Delta(\mathbf{r})$ is proportional to the superconducting pair wave function, and $V(\mathbf{r})$ is the position-dependent electron-electron interaction. The kernel $Q(\mathbf{r}-\mathbf{r}')$ can be represented in the form [12:(A5) and 12:(A6)],

$$Q(\mathbf{r}-\mathbf{r}') = (2\pi)^{-3} \int d^3q e^{i\mathbf{q}\cdot(\mathbf{r}-\mathbf{r}')} Q(\mathbf{q}), \quad (A2)$$

$$Q(\mathbf{q}) = T \sum_{\nu=-\infty}^{\infty} (2\pi)^{-3} \int d^3p Q_{\omega}(\mathbf{p}, \mathbf{q}-\mathbf{p}), \quad (A3)$$

where $\omega = (2\nu+1)\pi T$. The quantity $Q_{\omega}(\mathbf{p}, \mathbf{q}-\mathbf{p})$ satisfies an integral equation, in the presence of impurities. For

²⁹ M. P. Sarachik, E. Corenzwit, and L. D. Longinotti, Phys. Rev. **135**, A1041 (1964).

³⁰ K. Schwidtal, Z. Physik **158**, 563 (1960).

nonmagnetic impurities this integral equation is given by 12:(A7), while for impurities with spin which exchange-scatter, Abrikosov and Gor'kov have shown that the integral equation becomes Ref. 23 Eq. (19) [to be denoted 23:(19)]

$$Q_{\omega}(\mathbf{p}, \mathbf{q}-\mathbf{p}) = \bar{G}_{\omega}(\mathbf{p}) \bar{G}_{-\omega}(\mathbf{q}-\mathbf{p}) \left[1 + n(2\pi)^{-3} \int d^3 p' \times (|u_1|^2 - |u_2|^2) Q_{\omega}(\mathbf{p}', \mathbf{q}-\mathbf{p}') \right]. \quad (\text{A4})$$

The impurity concentration is n , while u_1 and u_2 are the spin-independent and spin-flip scattering amplitudes, respectively. The one-electron propagator is [23:(14)]

$$\bar{G}_{\omega}(\mathbf{p}) = [i\omega - (\mathbf{p}^2/2m) + \mu + i \operatorname{sgn}\omega/2\tau], \quad (\text{A5})$$

and we introduce the scattering times

$$1/2\tau \equiv \pi n N(0) (|u_1|^2 + |u_2|^2), \quad (\text{A6})$$

$$1/2\tau_s \equiv \pi n N(0) |u_2|^2 \ll 1/2\tau.$$

Since u_1 and u_2 are assumed to be constants, Eq. (A4)

may be solved trivially; substituting into Eq. (A3) leads to

$$A(\mathbf{q}) = T \sum_{\nu} R(q) / [1 - n(|u_1|^2 - |u_2|^2) R(\mathbf{q})], \quad (\text{A7})$$

where

$$R(\mathbf{q}) \equiv (2\pi)^{-3} \int d^3 p \bar{G}_{\omega}(\mathbf{p}) \bar{G}_{-\omega}(\mathbf{q}-\mathbf{p}). \quad (\text{A8})$$

Substituting expression (A5) into (A8), the evaluation of $R(\mathbf{q})$ can be carried out, yielding [12:(A11)]

$$R(\mathbf{q}) = (2\pi N(0)/\nu_F q) \tan^{-1}(\nu_F q / [2|\omega| + (1/\tau)]). \quad (\text{A9})$$

For dirty materials where $q l \ll 1$, we may expand $R(\mathbf{q})$; substituting into Eq. (A7) leads to

$$Q(\mathbf{q}) = N(0) \left\{ \ln \frac{1.14 \Theta_D}{T} - \chi \left(\frac{q^2 \nu_F l}{6\pi\tau} + \frac{1}{2\pi T \tau_s} \right) \right\}. \quad (\text{A10})$$

Comparing Eq. (A10) with the previous analysis of Werthamer¹² in the nonmagnetic case completes the derivation of Eq. (7) in the text.

Optical Second-Harmonic Generation Using a Focused Gaussian Laser Beam*

J. E. BJORKHOLM

Microwave Laboratory, Stanford University, Stanford, California

(Received 27 September 1965)

This paper reports analytical and experimental results on optical second-harmonic generation in the focus of the lowest order transverse mode of a cw gas laser beam. The results of the calculation are explained in physical terms and are confirmed by experiments carried out in crystals of ammonium dihydrogen phosphate (ADP). The dependence of the second-harmonic power generated in a negatively birefringent crystal upon the crystal double-refraction angle and the divergence, or diffraction, of the focused beam is obtained. There are found to be four distinct asymptotic regions, determined by the ratios of the characteristic lengths z_R and l_a to the crystal length l , where the Rayleigh range of the focused beam z_R characterizes the focus, and l_a is characteristic of the crystal double-refraction angle α and the laser beam focal spot size w_0 . Proceeding from weak focusing to strong focusing (or in the direction of decreasing w_0), the second-harmonic power in the four regions varies as l^2/w_0^2 , $l/\alpha w_0$, w_0/α , and w_0^2 , respectively. There is an optimum degree of focusing, determined only by the crystal length, for which a maximum amount of second-harmonic power is generated. This degree of focusing corresponds to $z_R = l/\pi$, and the corresponding power which is generated depends upon both l and α . Optimum focusing in a crystal of ADP 1 cm long yields about 400 times more second-harmonic power than the collimated laser beam. The excellent agreement between analysis and experiment allows the accurate measurement of optical nonlinearities using focused beams. The results for the general case of a crystal anywhere along the focused beam are also presented. Interpretation of them shows that the limiting of second-harmonic generation by double refraction is determined by beam divergence, not beam radius.

I. INTRODUCTION

NONLINEAR optical effects are most readily detected when brought about by a beam of high-intensity light. For this reason, high-power Q -switched

ruby lasers and focused laser beams are often used in the study of such effects. In many cases, however, it is desirable to observe the nonlinear effects on a continuous basis. This necessitates the use of cw lasers, which are characterized by low power and hence low efficiency in inducing the desired nonlinear effects. For the case of optical second-harmonic generation (SHG), the technique of index matching must be employed in order to

* This work was supported by the Air Force Office of Scientific Research, United States Air Force, under Contract AF 49(638)-1525. The author is grateful to the Ground Systems Group of Hughes Aircraft Company for support furnished by a Hughes Doctoral Fellowship.